ChemComm

Cite this: *Chem. Commun.*, 2012, **48**, 738–740

www.rsc.org/chemcomm

COMMUNICATION

Label-free and sensitive thrombin sensing on a molecularly grafted aptamer on graphene†

Yanping Wang,[a] Yinghong Xiao,*[a] Xiaoling Ma,[b] Na Li[a] and Xiaodi Yang*[a]

Received 1st September 2011, Accepted 9th November 2011
DOI: 10.1039/c1cc15429j

A unique nanocomposite was constructed by grafting an aptamer on graphene and used as a label-free biosensor for thrombin sensing, showing good selectivity, a low detection limit of 0.45 fM and high sensitivity, with a linear response up to 100 fM.

Aptamers are able to bind a broad range of target proteins with high affinity and specificity.[1,2] It is facile for aptamers to convert bio-recognition events into physically detectable electrochemical signals. Thus, aptamer-based biosensors are considered as prospective sensors for rapid and sensitive protein detections. In recent reports, label-free electrochemical biosensors for the determination of proteins have attracted increasing attention because the labeling process of aptamers is time-consuming and leads to bioaffinity-reduction. Nanostructured materials have aroused increasing interest recently because at the nanoscale their physical and chemical properties can be significantly enhanced. The incorporation of nanomaterials into aptamers has been extensively studied to improve the sensitivity of sensors.[3–9]

As a new kind of carbon material, graphene (GR) possesses numerous unexpected properties, including high electrical conductivity, large surface area and good biocompatibility,[10–13] rendering it a candidate for use in electrochemical sensors. Several investigators reported their research on noncovalent assembly of GR and aptamers.[14,15] GR can be used to construct label-free and sensitive electrochemical aptasensors. However, such an investigation has never been carried out.

Electrochemical aptasensors prepared by covalent assembly against noncovalent assembly exhibit the following advantages. Firstly, the binding force between the aptamer and solid surface is improved, thus it is easy to form a stable modifying layer. Secondly, the distance between the redox compound and electrode surface is reduced, which in turn accelerates the electron transfer rate at the electrode/electrolyte interface. Here, we report a novel aptasensor by molecularly grafting thrombin-binding aptamer (TBA) on GR for label-free thrombin sensing.

The construction of the aptamer-grafted GR and its label-free aptasensor are schematically shown in Fig. 1. Chitosan (CS) was chosen as an adhesive molecule to immobilize graphene oxide (GO) on the surface of glassy carbon electrode (GCE) and the conversion of GO to GR was performed *via* chemical reduction. TBA was molecularly grafted onto GR *via* covalent binding. The sensing mechanism is also illustrated in Fig. 1. In the presence of the target molecule of thrombin, a complex of quadruplex-thrombin is formed and such a complex increases the steric hindrance that greatly restrains access of electrons for a redox probe of $[Fe(CN)_6]^{3-/4-}$.

To identify the material on the electrode surface, the Raman spectra of GO–GCE and GR–GCE shown in Fig. 2(A) were studied. The Raman spectra of both electrodes exhibit the presence of D and G bands. The D band at 1351 cm^{-1} arises from sp^3-hybridized carbon and the peak at 1594 cm^{-1} represents the E_{2g} zone center mode of the crystalline graphite.[16,17] It is seen that the integrated intensity ratio of the D and G bands (I_D/I_G ratio) of GR–GCE dramatically increases in comparison with that of GO–GCE, which are 1.30 and 0.86, respectively. The increase in the I_D/I_G ratio is induced by structural disorder, indicating the successful conversion from GO to GR. Surface characterization by FTIR was carried out to verify whether TBA was successfully grafted on GR. As shown in Fig. 2(B), compared with a GR-modified electrode, the GR–TBA modified electrode exhibits characteristic peaks at 3360 cm^{-1} and 967 cm^{-1}, which correspond to stretching vibrations of

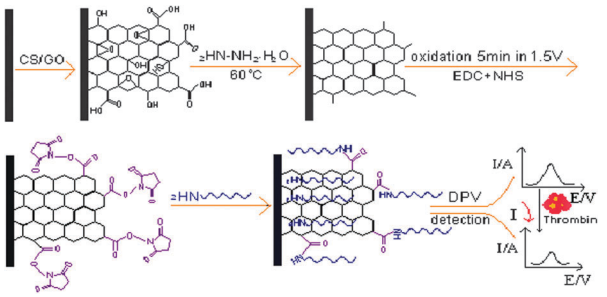

Fig. 1 A schematic diagram of the construction of the GR–TBA-based aptasensor and its sensing mechanism.

[a] *Jiangsu Key Laboratory of New Power Batteries, Jiangsu Key Laboratory of Biofunctional Materials, Laboratory of Electrochemistry, College of Chemistry and Material Science, Nanjing Normal University, Nanjing 210097, China. E-mail: yhxiao@njnu.edu.cn; Fax: +86 25-85891536; Tel: +86 25-85891536*
[b] *Nanjing Maternity and Child Health Care Hospital, Nanjing Medical University, Nanjing 210097, China. E-mail: yangxiaodi@njnu.edu.cn; Fax: +86 25-83598280; Tel: +86 25-83598648*

† Electronic supplementary information (ESI) available: Experimental details and some electrochemical measurements. See DOI: 10.1039/c1cc15429j

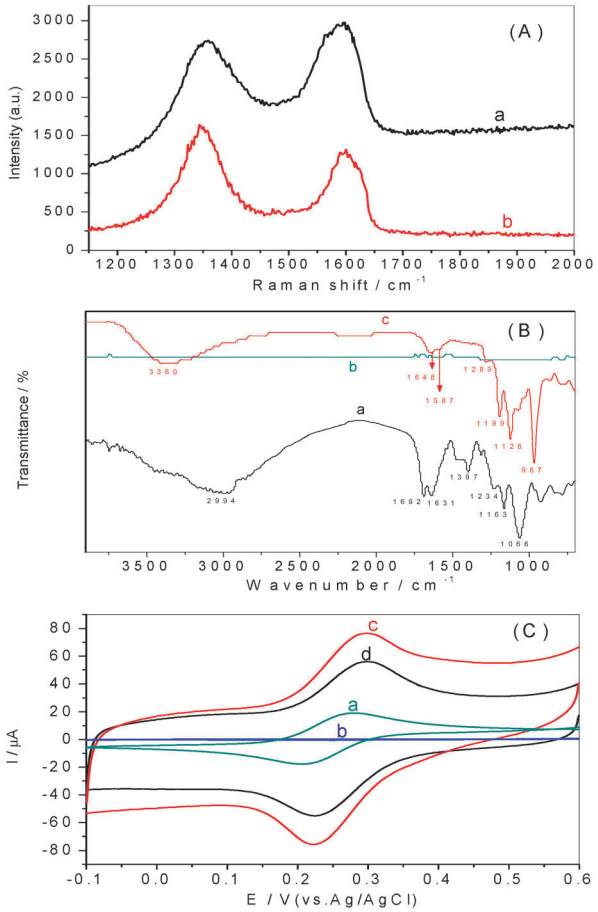

Fig. 2 (A) Raman spectra of GO–GCE (a) and GR–GCE (b). (B) ATR–FTIR spectra of TBA (a), GR–GCE (b), and GR–TBA–GCE (c). (C) CVs of bare GCE (a), GO–GCE (b), GR–GCE (c) and GR–TBA–GCE (d) in 0.10 M PBS (pH 7.4) containing 10 mM $K_3Fe(CN)_6/K_4Fe(CN)_6$ and 0.1 M KCl. Scan rate was 50 mV s^{-1}.

N–H and C–O–C for TBA, respectively. In addition, bands around 1648 cm^{-1} and 1587 cm^{-1} attributed to CO–NH for TBA can be clearly seen. These results clearly indicate the successful grafting of TBA on GR. The advantages of the use of GR are demonstrated in Fig. 2(C). The bare GCE exhibits a couple of redox peaks. Self-assembly of GO onto the electrode results in a CV in the shape of a straight line, due to the strong inhibition of the electron migration process caused by the great membrane resistance of GO film. After the GO-modified electrode was reduced, the CV of GR–GCE shows high peak currents. This is related to a high density of edge-plane-like defective sites in GR.[16] When TBA is grafted onto the surface of the GR functionalized electrode, the peak current decreases instead, indicating the formation of an organic layer of TBA. TBA with negative charges on its phosphate backbone repels $[Fe(CN)_6]^{3-/4-}$ redox couples to access the reactive centers on the electrode.[2] The CV curves in Fig. 2(C) show that GR greatly promotes the electron transfer. The ratio of the current density before and after the reduction of GO is 0.58.

Since the interaction of thrombin and TBA takes time, the effect of incubation time on sensor response was studied. Fig. 3 shows the dependence of current on incubation time. The plot in Fig. 3 tells us that the current response decreases with the

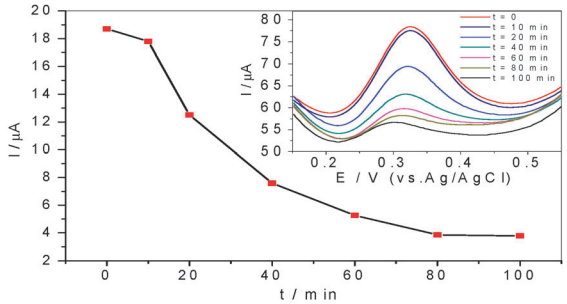

Fig. 3 The effect of incubation time on aptasensor response towards 50 pM thrombin in 0.10 M PBS (pH 7.4) containing 10 mM $K_3Fe(CN)_6/K_4Fe(CN)_6$ and 0.1 M KCl. Inset is the corresponding DPV curves.

incubation time from 10 to 80 min and reaches a plateau after 80 min, suggesting that the association reaction between aptamer and thrombin almost reaches saturation at 80 min. Nevertheless, considering the urgent time in clinical practice, 20 min is good enough because the response is almost half that of 80 min. Thus, 20 min was chosen as the incubation time for following experiments.

The response of the GR-based aptasensor towards different thrombin concentrations is shown in Fig. 4. The DPV curves in Fig. 4(A) show that the peak current gradually decreases with increasing concentrations of thrombin, which should be attributed to an increased electron transfer barrier for redox probes $[Fe(CN)_6]^{3-/4-}$ resulting from more bonded thrombin molecules on TBA. Note that the redox potential shifted to be negative with increasing thrombin concentrations. A possible explanation is that there are changes in the charged surface of

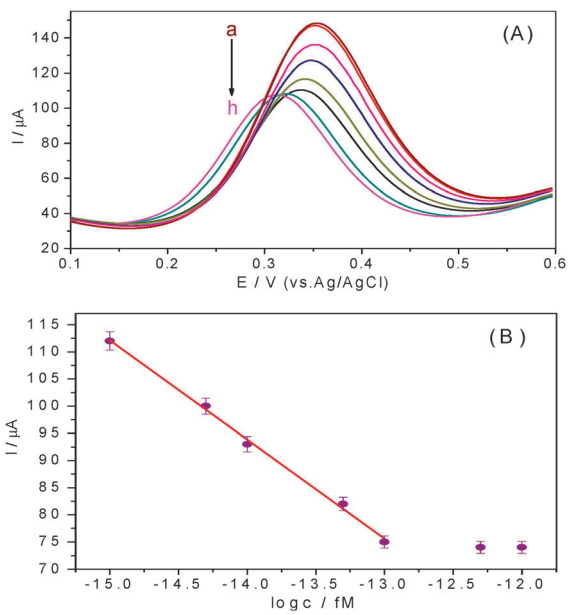

Fig. 4 (A) The relationship between the current response and α-thrombin concentration. The concentration of thrombin is 0 (a), 1 (b), 5 (c), 10 (d), 50 (e), 100 (f), 500 (g) and 1000 fM (h) in 0.10 M PBS (pH 7.4) containing 10 mM $K_3Fe(CN)_6/K_4Fe(CN)_6$ and 0.1 M KCl. Parameters for DPV pulse amplitude of 0.05 V, pulse width of 0.05 s and pulse period of 0.2 s. (B) The calibration curve between the current response and thrombin concentration (logarithm). The measurements were repeated 3 times to obtain the standard deviation.

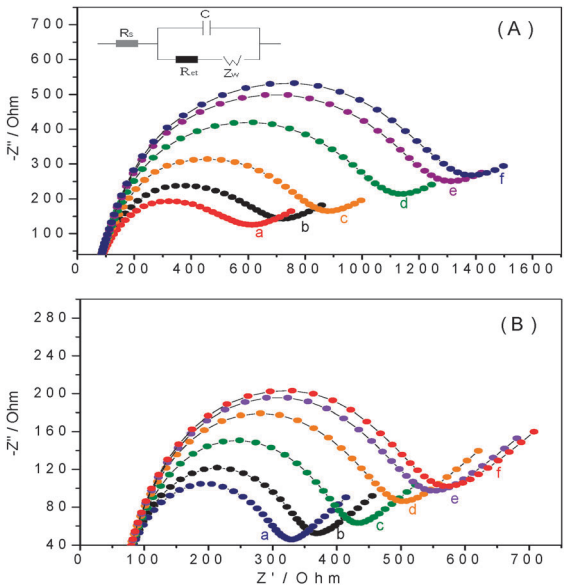

Fig. 5 Nyquist plots of Faradic impedance obtained in 0.10 M PBS (pH 7.4) containing 10 mM $K_3Fe(CN)_6/K_4Fe(CN)_6$ and 0.1 M KCl for GR–TBA–GCE (A) and TBA–GCE (B) for different thrombin concentrations of 0 (a), 1 (b), 5 (c), 10 (d), 50 (e) and 100 fM (f). Inset is a schematic of the equivalent circuit. R_s is the ohmic resistance of the electrolyte, R_{et} is the electron-transfer resistance, C is double-layer capacitance and Z_w is Warburg impedance.

the aptamer and its electronegativity may decrease upon interaction with thrombin. Thus, its repellence to $[Fe(CN)_6]^{3-/4-}$ redox probe is reduced, leading to a negative shift of the redox potential. The calibration curve by plotting the current response with thrombin concentration is presented in Fig. 4(B). It shows a good linear region with a concentration of thrombin in the range 1–100 fM. The linear relation has a regression equation of $A = -18.28a - 162.0$ with a correlation coefficient (R^2) of 0.9963, where A and a are the current response and the logarithm of thrombin concentration, respectively. A detection limit ($S/N = 3$) as low as 0.45 fM is observed, which is lower than 7.6×10^{-13} M previously reported.[18] We also investigated the application of the GR-based aptasensor in the detection of thrombin in healthy human serum samples. The current response was recorded for thrombin in varying concentrations in healthy human serum samples. Results were obtained at four prepared electrodes for 5 repetitive assays. A detection limit of 2.09 fM of thrombin in a real serum sample can be estimated, with a relative standard deviation of 1.41×10^{-6}, implying its higher sensitivity than the reported GR fluorescence aptasensor[14] and electrochemical thrombin sensors.[19]

To better understand the role of GR in the aptasensor, impedance behaviors of GR–TBA- and TBA-modified electrodes were studied under the same conditions. As illustrated in Fig. 5(A and B), both R_{et} value increased after two electrodes were immersed in thrombin solution. The difference is that the average growth rate of R_{et} for TBA–GCE is 8.41 Ohm fM^{-1}, while it is 15.34 Ohm fM^{-1} for GR–TBA–GCE, which is 1.82 times larger than that of TBA–GCE. This would greatly improve the sensitivity of the aptasensor.

While sensors with high sensitivity can detect an extremely low concentration of target molecules, those with good selectivity can efficiently eliminate various interferences in biological systems.[20] The selectivity of the GR–TBA-based aptasensor was also studied in proteins of bovine serum albumin (BSA) and trypsase (TYP) that always co-exist with thrombin in blood. The sensor shows a negligible response towards these proteins without thrombin, whereas a substantial drop in current is observed in solution containing thrombin, indicating the good selectivity of the aptasensor.

In conclusion, a unique nanocomposite was constructed by grafting an aptamer on GR and used as a label-free biosensor for thrombin sensing. The GR–TBA-based apasensor provides good selectivity, a low detection limit of 0.45 fM and high sensitivity towards thrombin, with a linear response up to 100 fM. The significant improvement comes from GR, which greatly speeds up the charge transfer of the sensing platform. This study provides a universal approach to use GR for constructing label-free electrochemical biosensors for the determination of various biological molecules.

This work was supported by the Priority Academic Program Development of Jiangsu Higher Education Institutions, the National Natural Science Foundations of China (No. 20875047) and the research funding of the MOE Key Laboratory of Analytical Chemistry for Life Science (No. KLACLS07006).

Notes and references

1 P. Kara, A. de la Escosura-Muñiz, M. Maltez-da Costa, M. Guix, M. Ozsoz and A. Merkoçi, *Biosens. Bioelectron.*, 2010, **26**, 1715.
2 Z. X. Zhang, W. Yang, J. Wang, C. Yang, F. Yang and X. R. Yang, *Talanta*, 2009, **78**, 1240.
3 X. X. Li, L. H. Shen, D. D. Zhang, H. L. Qi, Q. Gao, F. Ma and C. X. Zhang, *Biosens. Bioelectron.*, 2008, **23**, 1624.
4 S. Centi, S. Tombelli, M. Minunni and M. Mascini, *Anal. Chem.*, 2007, **79**, 1466.
5 M. McMullan, N. J. Sun, P. Papakonstantinou, M. X. Li, W. Z. Zhou and D. Mihailovic, *Biosens. Bioelectron.*, 2011, **26**, 1853.
6 H. Yang, J. Ji, Y. Liu, J. L. Kong and B. H. Liu, *Electrochem. Commun.*, 2009, **11**, 38.
7 H.-M. So, K. Won, Y. H. Kim, B.-K. Kim, B. H. Ryu, P. S. Na, H. Kim and J.-O. Lee, *J. Am. Chem. Soc.*, 2005, **127**, 11906.
8 A. Düzgün, A. Maroto, T. Mairal, C. O'Sullivan and F. X. Rius, *Analyst*, 2010, **135**, 1037.
9 Z. S. Wu, M. M. Guo, S. B. Zhang, C. R. Chen, J. H. Jiang, G. L. Shen and R. Q. Yu, *Anal. Chem.*, 2007, **79**, 2933.
10 C. L. Kane, *Nature*, 2005, **438**, 168.
11 D. Chen, L. H. Tang and J. H. Li, *Chem. Soc. Rev.*, 2010, **39**, 3157.
12 Y. Wang, Z. H. Li, J. Wang, J. H. Li and Y. H. Lin, *Trends Biotechnol.*, 2011, **29**, 205.
13 J. F. Che, L. Shen and Y. H. Xiao, *J. Mater. Chem.*, 2010, **20**, 1722.
14 H. X. Chang, L. H. Tang, Y. Wang, J. H. Jiang and J. H. Li, *Anal. Chem.*, 2010, **82**, 2341.
15 J. B. Liu, Y. L. Li, Y. M. Li, J. H. Li and Z. X. Deng, *J. Mater. Chem.*, 2010, **20**, 900.
16 M. Zhou, Y. M. Zhai and S. J. Dong, *Anal. Chem.*, 2009, **81**, 5603.
17 J. I. Paredes, S. Villar-Rodil, P. Solís-Fernández, A. Martínea-Alonso and J. M. D. Tascón, *Langmuir*, 2009, **25**, 5957.
18 X. M. Li, J. M. Liu and S. S. Zhang, *Chem. Commun.*, 2010, **46**, 595.
19 T. Sun, L. Wang, N. Li and X. X. Gan, *Bioprocess Biosyst. Eng.*, 2011, **34**, 1081.
20 C. X. Guo, X. T. Zheng, S. R. Ng, Y. C. Lai, Y. Lei and C. M. Li, *Chem. Commun.*, 2011, **47**, 2652.